ELSEVIER

Materials Science and Engineering B80 (2001) 266–269

MATERIALS SCIENCE & ENGINEERING B

www.elsevier.com/locate/mseb

Local absorption spectra of single and coupled semiconductor quantum dots

C.D. Simserides *, U. Hohenester, G. Goldoni, E. Molinari

Dipartimento di Fisica, Istituto Nazionale per la Fisica della Materia (INFM), Università di Modena e Reggio Emilia, Via Campi 213A, I-41100 Modena, Italy

Abstract

We study theoretically the local absorption spectra of single and double semiconductor quantum dots (QDs), in the linear regime. The three-dimensional confinement leads to an enhancement of the Coulomb correlations, while the spectra depend crucially on the size of the 'local' probe. We show that because of such Coulomb correlations the intensity of certain optical peaks as a function of the resolution can exhibit an unexpected non-monotonic behavior for spatial resolutions comparable with the excitonic Bohr radius. We finally discuss the optical near-field properties of coupled QDs for different coupling strengths.

Keywords: Semiconductors; Nanostructures; Local absorption; Coulomb correlations

1. Introduction

Recently, much attention has been devoted to semiconductor quantum dots (QDs) [1,2], where the three-dimensional confinement gives rise to a discrete atomic-like density of states. In turn, the coupling to the solid-state environment is suppressed and Coulomb correlations are strongly enhanced. For these reasons, QDs display a rich number of interesting and new physical phenomena, which make them particularly promising candidates for novel optoelectronic device applications [2]. However, despite the continuing progress, all the available fabrication approaches still suffer from the effects of inhomogeneity and dispersion in dot size, which lead to large line widths when optical experiments are performed on large QD ensembles. A major advancement in the field has come from different types of local optical experiments that allow the investigation of individual QDs thus avoiding inhomogeneous broadening [3–8]. Among local spectroscopies, near-field optical approaches [9] are especially interesting as they bring the spatial resolution well below the diffraction limit of light: with the development of small-aperture optical fiber probes, sub-wavelength resolutions were achieved ($\lambda/8$–$\lambda/5$ or $\lambda/40$) [10,11].

As the resolution increases, local optical techniques allow direct access to the space and energy distribution of quantum states within semiconductor nanostructures. Theoretically, the interaction between a given near-field probe and the carrier states inside the dots is not at all obvious: In analogy with ultrafast time-resolved spectroscopies that have revealed the importance of phase coherence in the quantum-mechanical time evolution of photoexcited carriers, it may be expected that spatial interference of quantum states plays a dominant role when variations of the electromagnetic (EM) field occur on an ultrashort length scale. By use of a microscopic model for computing carrier states in QDs and of a recently developed theoretical formulation of local optical absorption [12], in this paper, we quantitatively analyze optical near-field spectra for prototypical dot structures. The importance of accounting for non-locality and Coulomb interactions within a microscopic framework is highlightened at a few representative examples.

2. Theory in brief

In our calculations for the QD, we start from the single-particle energies $\epsilon^{\mathrm{e}}_{\mu}$ ($\epsilon^{\mathrm{h}}_{\nu}$) and wave functions $\phi^{\mathrm{e}}_{\mu}(\mathbf{r})$ ($\phi^{\mathrm{h}}_{\nu}(\mathbf{r})$) for electrons (holes), which we derive by

* Corresponding author.

0921-5107/01/$ - see front matter
PII: S0921-5107(00)00652-8

solving the single-particle Schrödinger equation within the envelope-function and effective-mass approximations [13,14]. When the semiconductor nanostructure is perturbed by an external light field (e.g. laser), electron–hole pairs are created which propagate in the presence of the mutual Coulomb interaction and of the dot confinement potential. Restricting ourselves to the linear regime, the optical response is governed by the dynamics of a single electron–hole pair (exciton), where the electron–hole Schrödinger equation [15]:

$$(\epsilon_\mu^{\mathrm{e}} + \epsilon_\nu^{\mathrm{h}})\Psi_{\mu\nu}^{\lambda} + \sum_{\mu'\nu'} V_{\mu\mu',\nu\nu'}^{\mathrm{eh}} \Psi_{\mu'\nu'}^{\lambda} = E_\lambda \Psi_{\mu\nu}^{\lambda}, \tag{1}$$

provides the exciton energies E_μ and wave functions $\Psi_{\mu\nu}^{\lambda}$ (with real-space representation $\Psi^{\lambda}(\mathbf{r}_{\mathrm{e}},\mathbf{r}_{\mathrm{h}}) = \Sigma_{\mu\nu}\, \phi_\mu^{\mathrm{e}}(\mathbf{r}_{\mathrm{e}})\Psi_{\mu\nu}^{\lambda}\phi_\nu^{\mathrm{h}}(\mathbf{r}_{\mathrm{h}})$; here, $V_{\mu\mu',\nu\nu'}^{\mathrm{eh}}$ are the electron–hole Coulomb elements which are responsible for Coulomb-induced renormalizations in the optical spectra.

The EM field $\mathscr{E}(\mathbf{r},\omega)$ of the near-field probe induces an interband polarization $P(\mathbf{r},\omega)$, which in linear response, is related to $\mathscr{E}$ through the non-local electric susceptibility [12]:

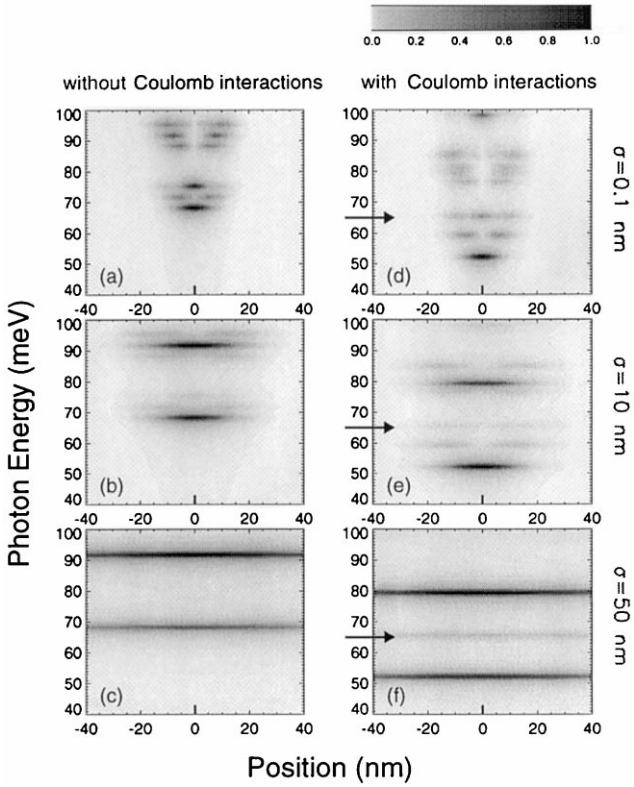

Fig. 1. Local absorption spectra $\alpha_\xi(X,\hbar\omega)$ for a single QD with ((d)–(f) and with out ((a)–(c)) Coulomb interactions and for different values of σ; here, the tip is swept along the x-direction (with $y = 0$), i.e., passing through the center of the QD. Photon energy is measured with respect to the band gap. In this calculations, we used a basics of 6 electron and hole states, respectively.

$$\chi(\mathbf{r},\mathbf{r}';\omega) = \mu_0^2 \sum_\lambda \frac{\Psi^{\lambda}(\mathbf{r},\mathbf{r})\Psi^{\lambda *}(\mathbf{r}',\mathbf{r}')}{E_\lambda - \hbar\omega - i\gamma}, \tag{2}$$

where μ_0 is the bulk dipole element, and the small damping constant γ accounts for the finite lifetime of exciton states due to environment coupling (e.g., phonons; we use $\gamma = 1$ meV). For the EM field distribution, it is convenient to consider a given profile $\xi(\mathbf{r}-\mathbf{R})$ centered around the near-field tip position $\mathbf{R}$, and the local absorption spectrum at position $\mathbf{R}$ can be expressed in its final form [12]:

$$\alpha_\xi(\mathbf{R},\omega) \propto \Im \sum_\lambda \frac{\alpha_\xi^{\lambda}(\mathbf{R})}{E_\lambda - i\gamma - \hbar\omega}, \tag{3}$$

where $\alpha_\xi^{\lambda}(\mathbf{R}) = \left|\int d\mathbf{r}\Psi^{\lambda}(\mathbf{r},\mathbf{r})\xi(\mathbf{r}-\mathbf{R})\right|^2$. Two limiting cases can be readily identified in Eq. (3): For a spatially homogeneous EM field (far-field), the oscillator strength α_ξ^{λ} is given by the spatial average of the excitonic wave function; in the opposite limit of an infinitely narrow probe, one is probing the local value of the exciton wave function. Within the intermediate regime of a narrow but finite probe, $\Psi^{\lambda}(\mathbf{r},\mathbf{r})$ is averaged over a region which is determined by the spatial extension of the light beam; therefore, excitonic transitions which are optically forbidden in the far-field may become visible in the near-field.

3. Results and discussion

Fig. 1 reports the calculated local absorption spectra $\alpha_\xi(X,\hbar\omega)$ for a single QD with a prototypical dot confinement, which is parabolic in the (x, y)-plane and box-like along the z-axis[1]. *For* ξ, we use a Gaussian with $\xi(x, y, z) \propto \exp -(x^2+y^2)/2\sigma^2$ (values of σ are shown on the right-hand side of Fig. 1; because of the narrow well width of the dot confinement,[1] the z-dependence of the EM near-field profile is neglected). The Gaussian acts as an envelope on Ψ^{λ}. The spatial resolution of the EM field distribution is then approxi-

[1] For the in-plane confinement potential, we use for a single dot $V_{\parallel}^{\mathrm{e,h}}(x,y) = \frac{1}{2}\mathscr{K}_{\mathrm{e,h}}(x^2+y^2)$, and for two dots (i.e., double dot) separated by distance d:

$$V_{\parallel}^{\mathrm{e,h}}(x,y) = \begin{cases} 1/2\mathscr{K}_{\mathrm{e,h}}\left(\left(|x| - \dfrac{d}{2}\right)^2 + y^2\right) & \text{for} |x| > \dfrac{d}{4} \\ 1/2\mathscr{K}_{\mathrm{e,h}}\left(\left(\dfrac{d^2}{8} - x^2\right) + y^2\right) & \text{otherwise} \end{cases}$$

with $\mathscr{K}_{\mathrm{e,h}} = m_{\mathrm{e,h}}(\omega_0^{\mathrm{e,h}})^2$, and $\hbar\omega_0^{\mathrm{e,h}}$, the level splittings of the in-plane harmonic potential (such confinement potentials have been demonstrated to be a good approximation for self-assembled quantum dots formed by strained-layer epitaxy [1]). In our calculations, we set $\hbar\omega_0^{\mathrm{e}} = 20$ meV, $\hbar\omega_0^{\mathrm{e}} = 3.5$ meV (with this choice, electron and hole wave functions have the same lateral extension), and the well-width in z-direction is 10 nm; material parameters for GaAs/AlGaAs are used.

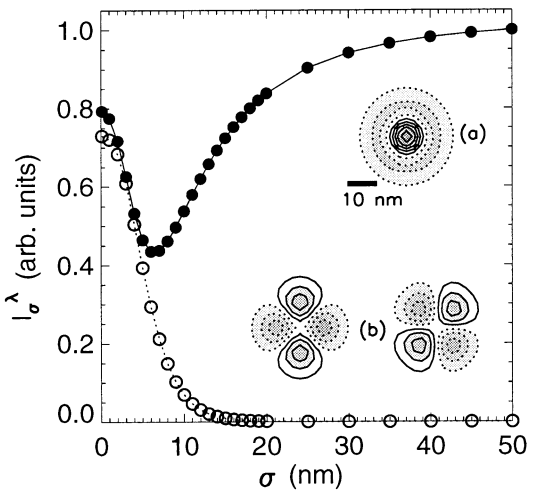

Fig. 2. The relative contribution I_ξ^λ as a function of σ, of the exitons which are responsible for the non-monotonic behavior of the feature at 65 meV in Fig. 1 (see arrows). Inset: Contour plot of the wave functions of these exitons, $\Psi^\lambda(\mathbf{r},\mathbf{r})$ (solid and dashed lines correspond to positive and negative values, respectively): Full (open) circles correspond to exciton (a) (excitons (b)).

mately given by the full-width at half maximum (FWHM) of the Gaussian (i.e., $2\sqrt{2\ln 2}\sigma \approx 2.35\sigma$). Since the extension of the quantum states under present investigation is of the order of a few tens of nanometers, one can consider three different characteristic regimes of spatial resolution: (i) a regime where the FWHM is much larger than the extension of the quantum states (we use $\sigma = 50$ nm); (ii) a regime where the FWHM is comparable to the extension of the relevant quantum states (we use $\sigma = 10$ nm); and (iii) a regime with an extremely narrow probe beam (we use $\sigma = 0.1$ nm). This latter physically rather unrealistic regime provides a direct measure of the exciton wave functions. Finally, we notice that for GaAs the excitonic Bohr radius is ≈ 12 nm. By inspecting Fig. 1, we first emphasize the spectrally narrow and atomic-like features which are characteristic for semiconductor QDs. For the case of the highest spatial resolution, these features only extend over the region where the exciton is confined. A comparison of Fig. 1(a)–(c) with Fig. 1(d)–(f) reveals that Coulomb interaction induces several pronounced effects: (i) an almost rigid redshift of the spectra (due to the attractive electron–hole Coulomb interactions); (ii) a transfer of oscillator strength from transitions at higher energies to those at lower energies (see also Ref. [8]); and (iii) the appearance of new features in the optical spectra (see e.g. the features indicated by arrows at photon energy ≈ 65 meV). Varying σ, these features show an interesting non-monotonic behavior (in contrast to the other transitions which, with increasing σ, either remain strong or gradually disappear): They are quite strong at $\sigma = 0.1$ nm (Fig. 1(d)), almost disappear at $\sigma = 10$ nm (Fig. 1(e)), and become visible again in the far-field limit (Fig. 1(f)).

To understand the origin of this unexpected non-monotonic behavior, we analyze below the exciton states which contribute to the near-field spectra in slightly more detail. To facilitate our discussion, we introduce $I_\xi^\lambda \propto \int \mathrm{d}\mathbf{R}\ \alpha_\xi^\lambda(\mathbf{R})$, which provides a measure of the relative contribution of each exciton to the absorption spectra. Fig. 2 shows I_ξ^λ for the three excitons within the energy region of 65 meV (see arrows in Fig. 1). We observe that with increasing σ, the contribution of two of these excitons vanishes (open circles), whereas the contribution of the third exciton displays a non-monotonic behavior (full circles). The insets (a) and (b) of Fig. 2 show a contour plot of the wave functions of these excitons, $\Psi^\lambda(\mathbf{r},\mathbf{r})|_{z=0}$.

We notice that for a single parabolic QD, the single-particle eigenfunctions $\phi^{\mathrm{e,h}}$ are known analytically (Fock–Darwin states) [1]. In the following, we use the numbers 1,2,… for the radial quantum number and the letters s, p,… for the angular momentum in z-direction. Inspection of the wave functions $\Psi_{\mu\nu}^\lambda$ reveals that the largest contribution to exciton (a) (with 's-type symmetry') steams from the transition between the 1s state of electrons and the 2s state of holes. However, because of the Coulomb coupling, there is also a noticeable contribution from the 1s–1s and 1p–1p electron–hole transitions. In fact, these latter contributions are responsible for far-field coupling to the light field. On the other hand, the excitons (b) have apparently 'p-type symmetry'.

We furthermore find that the space average $\int \mathrm{d}\mathbf{r}\ \Psi^\lambda(\mathbf{r},\mathbf{r})$, which is responsible for the far-field optical selection rules, is non-zero only for exciton (a). Increasing σ, the spot area within which Ψ^λ is averaged increases. Hence, the 'p-type' functions are expected to vanish monotonically. On the contrary, for the 's-type' exciton there exists an optimal cancellation when the FWHM of the EM field distribution (i.e. $\approx 2.35\sigma$) becomes equal to the Bohr radius. Accordingly, we obtain the non-monotonic σ-dependence shown in Fig. 1. In spite of the specific carrier states of a single parabolic QD, we expect that such non-monotonic behavior appears quite generally in semiconductor nanostructures where carrier states are confined on a length scale comparable to the Bohr radius. This effect provides a striking fingerprint of Coulomb correlations in the optical near-field spectra. Indeed, we also find similar behavior in our calculations for the near-field spectra of coupled QDs [16].

Fig. 3(a) shows calculated far-field absorption spectra (i.e. $\alpha_\xi(\omega)$ for $\sigma \to \infty$) for a double dot[1,2] and for

[2] Coupled dots naturally occur in samples with dense QD packing, and have also been proposed for possible solid-state implementations of quantum-information processing.

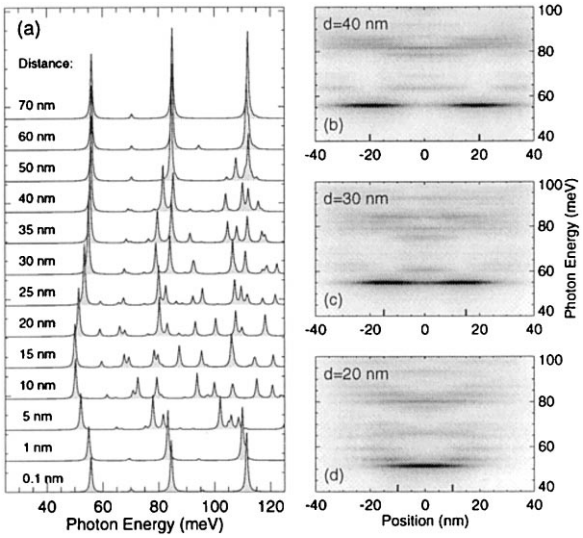

Fig. 3. Absorption spectra for a double dot: (a) varying the inter-dot distance, d, and using homogeneous EM field profile (i.e. far field; (b)–(d) near field absorption spectra for $\sigma = 10$ nm and a characteristic interdot distance (b) $d = 40$ nm, (c) $d = 30$ nm, and (d) $d = 20$ nm. we use a basics of 12 electron and hole states, respectively.

different interdot distances d. If the two dots are well separated ($d \sim 70$ nm), the spectrum closely resembles that of a single dot (Fig. 1(f)). Decreasing the interdot distance d, the peaks at higher photon energies (e.g. the peak multiplets at photon energies ~ 110 and ~ 80 meV) split because of the increased inter-dot coupling. This behavior is reflected much clearer in the near-field spectra of Fig. 3(b)–(d) ($\sigma = 10$ nm). Indeed, we observe a transition from a system where the low-energy exciton states are almost localized in the spatially separated minima of the two dots, to a system where the electron–hole states extend over the whole nanostructure. In particular for the ground-state exciton, we observe a splitting into a 'bonding' and 'anti-bonding' state. Because of symmetry, in the optical far-field only the symmetric ground-state exciton couples to the light field. Thus, Fig. 3 clearly reflects the formation of an 'artificial molecule' from two 'artificial atoms'.

In conclusion, we have presented a theoretical analysis of local absorption in single and coupled semiconductor QDs. The carrier states and the optical properties have been accounted for within a microscopic description. We have discussed the role of the spatial resolution of the optical near-field probe, and the important role of Coulomb interactions. For the case of a single QD, we have observed-with increasing resolution – a non-monotonic dependence of certain features in the optical spectra, which has been identified as a general fingerprint of Coulomb correlations in low-dimensional nanostructures. Finally, for two dots, we have discussed the formation of an 'artificial molecule'.

Acknowledgements

This work was supported in part by the EU under the TMR Network 'Ultrafast' and the IST Project SQID, and by INFM through grant PRA-SSQI. U.H. acknowledges support by the EC through a TMR Marie Curie Grant.

References

[1] L. Jacak, P. Hawrylak, A. Wojs, Quantum Dots, Springer, Berlin, 1998.
[2] D. Bimberg, M. Grundmann, N. Ledentsov, Quantum Dot Heterostructures, Wiley, New York, 1998.
[3] H.F. Hess, et al., Science 264 (1994) 1740.
[4] F. Flack, et al., Phys. Rev. B 54 (1996) R17312.
[5] T.D. Harris, et al., Appl. Phys. Lett. 68 (1996) 988.
[6] A. Richter, et al., Phys. Rev. Lett. 79 (1997) 2145.
[7] L. Landin, et al., Science 280 (1998) 262.
[8] A. Chavez-Pirson, et al., Appl. Phys. Lett. 72 (1998) 3494.
[9] M.A. Paesler, P.J. Moyer, Near-Field Optics: Theory, Instrumentation, and Applications, Wiley, New York, 1996.
[10] T. Saiki, K. Matsuda, Appl. Phys. Lett. 74 (1999) 2773.
[11] E. Betzig, J.K. Trautman, T.D. Harris, J.S. Weiner, R.L. Kostelak, Science 251 (1991) 1468.
[12] O. Mauritz, G. Goldoni, F. Rossi, E. Molinari, Phys. Rev. Lett. 82 (1999) 847.
[13] F. Rossi, E. Molinari, Phys. Rev. Lett. 76 (1996) 3642.
[14] F. Rossi, E. Molinari, Phys. Rev. B 53 (1996) 16462.
[15] U. Hohenester, E. Molinari, Phys. Stat. Sol. (a) 178 (2000) 277.
[16] C.D. Simserides, U. Hohenester, G. Goldoni, E. Molinari, Phys. Rev. B 62 (2000) 13657.